Particle Accelerators
submitted 1997

METHODS OF BOUNDING LONG TERM STABILITY IN STORAGE RINGS BY ESTIMATING PSEUDO INVARIANTS OF NONLINEAR MOTION

GEORG H. HOFFSTÄTTER

Institute of Applied Physics, University of Darmstadt, 64289 Darmstadt,Germany

MARTIN BERZ*

MSU/NSCL, East Lansing, MI 48824, USA

The problem of stability of weakly nonlinear dynamics originally arose in the perturbative analysis of planetary motion. Nowadays it is of great importance for the dynamics in storage rings. We use a method which we call pseudo invariant estimation (PIE). This method is influenced by the basic concepts of Ljapunov stability theory and Nekhoroshev's work on exponential estimates[1], which was introduced in a slightly different framework to the accelerator field by Warnock[2]. In our case the pseudo invariants needed for this approach are computed via nonlinear perturbative normal form theory. Various refinements of the method are analyzed, and several examples yielding practically relevant results are given. Furthermore, quantities can be computed that lead to novel criteria for accelerator design and optimization.

KEY WORDS: stability, nonlinear dynamics, Nekhoroshev, Lyapunov

1 INTRODUCTION

The methods by which long term stability in storage rings has traditionally been analyzed can roughly be divided into two groups; some methods use element–by–element tracking and others use the one turn map of the ring. The methods which use the one turn map can also be divided into two groups: some of these methods iterate the one turn map several times to obtain effects of many turns, other methods use the one turn map only once without iteration to directly extract the information relevant to the stability question. This situation can be summarized as follows:

* Supported in part by the National Science Foundation, Grant Number PHY 89-13815, and the Alfred P. Sloan Foundation

1. Element–by–element tracking	One turn map $\vec{M}$	
	2. $\vec{M}$ tracking	3. One application of $\vec{M}$

In principle the one turn transfer map, relating initial phase–space coordinates $\vec{z}_i$ to final coordinates after one turn by $\vec{z}_f = \vec{M}(\vec{z}_i)$ contains all information about the long term motion. This transfer map can also depend on n_p parameters δ_i, $i \in \{1, \ldots, n_p\}$ of the physical system involved, leaving $\vec{z}_f = \vec{M}(\vec{z}_i, \vec{\delta})$. Sometimes an appropriate choice of B–spline functions and Fourier series has been applied[3] to approximate a transfer map; more commonly the Taylor expansion of the function is used. In a differential algebra framework the Taylor map can be obtained to arbitrary order[4]. There are advantages and disadvantages associated with each of these approaches, which roughly can be summarized as follows:

1. + Easy to implement. Good for cross checking with other methods.
   - Very time consuming if a realistic number of turns should be tracked. Approximations have to be made to speed up programs. Stability of motion can only be checked for a limited number of particles. Computational inaccuracies can build up to an intolerable amount.
2. + The transfer maps of individual particle optical elements can be taken into account accurately. Lumping the influence of many optical elements into a single map can save time substantially.
   - Time considerations restrict calculations to about order twelve[5]. Applying the one turn map the required number of turns is very time consuming. The stability of only a limited number of phase space points can be analyzed. Computational errors can build up to such an extent that results are not trustworthy.
3. + No build up of computational error. Whole regions in phase space can be analyzed in their entirety. Computation is not iterative and can thus be easily parallelized.
   - Nontrivial computational environment for map computation and manipulation is needed. Predictions of stability times tend to be pessimistic.

The method studied here, which we call pseudo invariant estimation (PIE)[2] for reasons soon to become obvious, is of the third type. We will introduce the PIE method by using pseudo invariants of nonlinear normal form theory. This method comes close to giving guaranteed lower bounds on the survival time. The method was implemented in and the examples of this paper were computed with COSY INFINITY[6]. In the applications which will be presented, the specific dynamical system is a particle moving in an accelerator or storage ring. Partial derivatives, and therefore the Taylor expansions of the transfer maps, can be computed by the so–called DA method[7].

Normal form theory will provide functions f which are invariants of the map $\vec{M}$ up to order $n+1$ and thus $f \circ \vec{M} =_{n+1} f$. For the weakly nonlinear dynamics exhibited by particle motion close to the central orbit of an accelerator, these functions are approximate invariants, or pseudo invariants, of the transfer map.

For the PIE method, a suitable pseudo invariant test function f will be found which is chosen such that $f(\vec{z})$ is a measure of the distance between a particle with coordinates $\vec{z}$ and the central orbit. At this orbit, $f(\vec{z}) = 0$ and $\mathcal{A} = \{\vec{z}|f(\vec{z}) \leq \epsilon\}$ is a volume in phase space which contains the origin. In one turn around the ring the so described distance from the origin changes by $d_f(\vec{z}) = f(\vec{M}(\vec{z})) - f(\vec{z})$.

If the maximum δ of d_f on the phase space volume $\mathcal{A}$ can be found, it can be said with certainty how far a particle can move away from the closed orbit in one turn. It can also be stated rigorously that particles in the phase space volume $\mathcal{O}$ with $\mathcal{O} = \{\vec{z}|f(\vec{z}) \leq \epsilon - N\delta\}$ will not leave the volume $\mathcal{A}$ for N applications of the map. Analyzing the prospects of this approach is the main subject of this paper.

A section about normal form theory provides an overview over our choice of obtaining pseudo invariants. The importance of resonances and their influence on estimates of the survival time is discussed. Two refinements will be introduced which increase the obtainable bounds on long term stability. Furthermore, the theory is extended to maps which depend on unknown parameters.

1.1 History

The stability of planetary motion has been an important question for over a century. After early attempts by Laplace and Lagrange to understand the stability of the solar system, Poincaré[8], Birkhoff[9], and Siegel[10,11], among others, investigated the problem in detail. Usually the problem of planetary motion was analyzed by considering it as a perturbation of a known and solvable Hamiltonian system. Innovative studies of this problem were made by Kolmogorov[12], Arnol'd[13], and Moser[14]. Nekhoroshev formulated a theory which estimates the time of stability of a system with a perturbation strength proportional to ϵ by an exponential estimate[1]. He proves the following theorem: (citation from p. 4) "Suppose that H_0 satisfies certain steepness conditions, ... Then there are positive constants a, b, and ϵ_0 with the following property. Let $0 < \epsilon < \epsilon_0$. Then for every solution $I(t), \phi(t)$ of the system with the Hamiltonian $H_0(I) + \epsilon H_1(I, \phi)$, $|I(t) - I(0)| < \epsilon^b$ for all $t \in [0, T]$, where $T = \frac{1}{\epsilon} \exp(\frac{1}{\epsilon^a})$."

The proof involves succesive canonical transformations $(I, \phi) \to (J, \psi)$ in order to minimize the dependence of the Hamiltonian on ψ as much as possible, thus bringing the new coordinates J as close to invariants of motion as possible, a technique referred to as the creation of "almost integrals"[1,p. 21]. The exponential estimate is established by analyzing these canonical transformations, which are performed in a perturbative way with respect to ϵ, and by finding the optimum order to which a transformation should be performed.

For certain problems concerned with general Hamiltonians, celestial mechanics, and also single particle motion in accelerators[15], the Nekhoroshev method of exponential estimates has been used by finding values a and b.

The idea of the proof of the Nekhoroshev estimate has prompted an analysis of stability of the nonlinear motion in particle accelerators by analyzing it in normal form space, a space in which the Hamiltonian has little dependence on ψ to start with. In this space the change of the "almost integrals" or pseudo invariants is not

estimated by bounding the series of canonical transformations, but by performing the canonical transformations on the computer and then evaluating their effect on the pseudo invariants. This possibility was first mentioned and programmed by R. L. Warnock for maps obtained by interpolating individual tracking points.

Later it was realized that Hamiltonians are not needed when the one–turn map or Poincaré map of a storage ring is known[16,17]. One only has to find the maximum change δ of the nearly invariant function during one application of the transfer map of the accelerator. This maximum change over the relevant regions of phase space bounds the change of the pseudo invariant for the entire particle motion in this region. Several other improvements on the method of pseudo invariants were made; they include using maps which describe many turns in the accelerator and different means of finding canonical transformations to the pseudo invariant coordinates[18,19,2].

In the following our approach to the PIE method will be described in detail and applied to several examples, which will demonstrate the applicability and usefulness of the method[20]. This approach can be made completely rigorous by novel arithmetic allowing automatic result verification[21,22].

2 PSEUDO INVARIANT ESTIMATION (PIE)

As mentioned in the introduction, the PIE method analyzes the one–turn map directly without tracking through it several times, which in particular avoids computational inaccuracies. Furthermore this method does not only test single particles but provides information about all particles in a given region of phase space.

We assume that there is a closed orbit in the ring. Particles with phase space coordinates sufficiently near the closed orbit will be able to go around the ring once without collisions with the wall, while particles that are too far away from the closed orbit will be lost during one revolution. We therefore divide the phase space $\mathcal{P}$ into the allowed region $\mathcal{A}$ and the forbidden region $\mathcal{P}\backslash\mathcal{A}$.

The question we want to answer is: How many turns does a particle which originates in a given region of phase space $\mathcal{O}$ circle the ring without leaving the accelerator. We therefore look for the number

$$N_{\max} = \max\{n | \vec{M}^n(\mathcal{O}) \subseteq \mathcal{A}\} \ , \tag{1}$$

where $\vec{M}^n(\mathcal{O}) = \{\vec{M}^n(\vec{z}) | \vec{z} \in \mathcal{O}\}$, and $\vec{M}^n(\vec{z})$ stands for n applications of $\vec{M}$. The different regions are shown in Fig. 1(a). With the following method we will find a strict lower bound N for $N_{\max}$.

If we find a real–valued test function f that does not have common values in $\mathcal{O}$ and in $\mathcal{P}\backslash\mathcal{A}$, then successive action of the map must bridge a gap Δf as shown in Fig. 1(b) in order to map a $\vec{z} \in \mathcal{O}$ into $\mathcal{P}\backslash\mathcal{A}$. Particles start to bridge this gap by entering the phase–space region $\mathcal{S}_i = \vec{M}(\mathcal{O})\backslash\mathcal{O}$. The gap is bridged when a particle has reached the region $\mathcal{S}_f = \vec{M}(\mathcal{A})\backslash\mathcal{A}$. If $\mathcal{S}_i$ or $\mathcal{S}_f$ are empty, particles in $\mathcal{O}$ will never leave $\mathcal{A}$. If they are not empty, the gap goes from f_i to f_f with

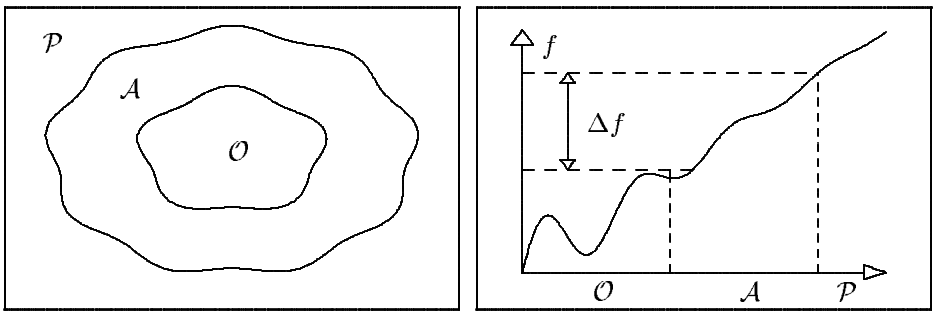

FIGURE 1: The left figure (a) shows the initial region $\mathcal{O}$ and the allowed region $\mathcal{A}$ of phase space $\mathcal{P}$ with $\mathcal{O} \subset \mathcal{A} \subset \mathcal{P}$. In the right figure (b) the gap Δf that has to be bridged is shown.

$f_i = \max\{f(\vec{z})|\vec{z} \in \mathcal{S}_i\}$ and $f_f = \min\{f(\vec{z})|\vec{z} \in \mathcal{S}_f\}$. The function

$$d_f = f(\vec{M}) - f \tag{2}$$

describes how much f deviates from being an invariant of the map $\vec{M}$; d_f is called deviation function. When a phase space point $\vec{z}$ is mapped through $\vec{M}$ once, the gap Δf is diminished by $d_f(\vec{z})$. If we assume $f_f \geq f_i$, the step from f_i towards f_f is always smaller or equal to

$$\delta = \max\{d_f(\vec{z})|\vec{z} \in (\mathcal{A}\backslash\mathcal{O})\} \quad . \tag{3}$$

A particle that starts in $\mathcal{O}$ therefore survives at least N turns, where

$$N = \mathrm{Int}[\frac{\mathrm{f_f} - \mathrm{f_i}}{\delta}] \leq \mathrm{N_{max}} \quad . \tag{4}$$

We are thus left with four problems:

1. finding a suitable test function f such that N becomes favorable,
2. finding f_i, the maximum of f on $\mathcal{S}_i$,
3. finding f_f, the minimum of f on $\mathcal{S}_f$,
4. finding δ, the maximum of the deviation function in the appropriate region.

To make the desired estimate as large as possible, we should find a function f which increases between the allowed and the forbidden region and should, at the same time, be close to an invariant of the one–turn map to make δ as small as possible.

The remaining three problems are concerned with finding maxima. These maxima can be found in a mathematically rigorous way in principle by using interval arithmetic; in practice, the computational effort turns out to be so horrendous that a totally new method based on the combination of DA and interval approaches named RDA was necessary to solve the problem[23].

Firstly one has to choose a suitable pseudo invariant f, and secondly we are faced with the problem of describing the phase–space regions $\mathcal{O}$ and $\mathcal{A}$ in a sensible way. We will use nonlinear normal form theory on Taylor maps to solve both problems[24,20].

3 NORMAL FORM TRANSFORMATIONS AND PSEUDO INVARIANTS

In the context of the PIE method we are only interested in the special case of stable linear motion, which means that all linear eigenvalues have modulus one. The phases of the linear eigenvalues λ_{2j-1} are the tunes ν_j of the system, where j refers to the different degrees of freedom.

If a map has tunes which are not in resonance to any order $m \leq n$, then one can find a transformation $\vec{B}$ which performs a nonlinear coordinate transformation such that the map in the new coordinates is a rotation up to order n. The radii are then invariants of motion up to order n. The procedure with which $\vec{B}$ is computed requires devision by resonance denominators

$$D_l(\vec{k}) = \exp(i2\pi\nu_l) - \exp(i2\pi \sum_{i=1}^{d} k_i \nu_i) \tag{5}$$

for a vector $\vec{k}$ of integers with $\sum_{i=1}^{2d} |k_i| \leq n$. At tune resonances, the resonance denominators below order $n+1$ vanish and the normal form transformation can not be performed. However, it is interesting to note that there is no problem with resonances when the map $\vec{M}$ is the Taylor map of a system which has d exact invariants of motion[20].

To illustrate the normal form transformation, the motion in phase space for 2000 turns in a typical accelerator is shown in Fig. 2(a). For each turn, the horizontal position x as well as its canonical conjugate momentum a is displayed. The finite width and the irregular structure of the band is a result of nonlinear effects and of coupling to the other degree of freedom, the motion in vertical direction. Fig. 2(b) shows the same motion after transformation by the normal form map.

4 EXAMPLES OF THE USE OF THE METHOD

The six following systems will be used to test the normal form invariants and the PIE method:

1. The physical pendulum of length one meter. We chose an emittance of $\epsilon = 10,000$ mm mrad and a tune of $\nu = 0.379$.
2. The Henon map for one degree of freedom for a kick strength of 1.1 and an emittance of $10,000$mm mrad for a tune of $\nu = 0.379$.

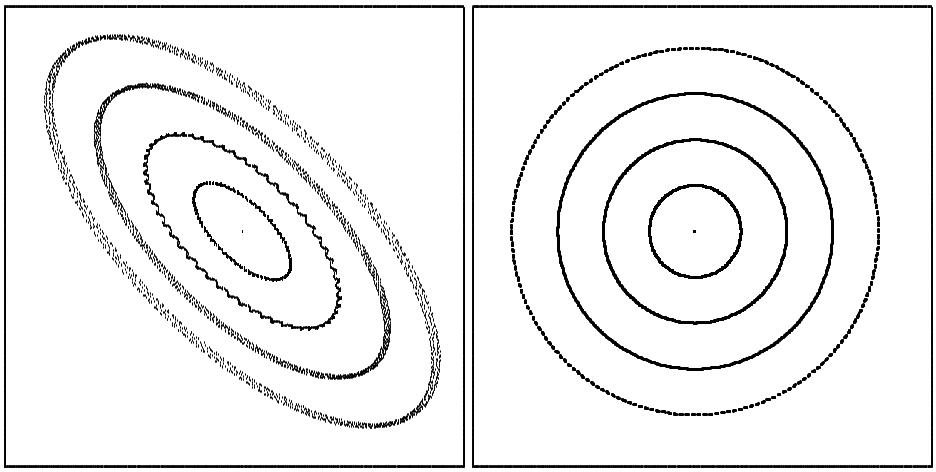

FIGURE 2: Phase diagram for 2000 turns in an accelerator for four initial conditions. The left picture shows the motion displayed in standard particle optical coordinates x and a, and the right picture shows the same motion in normal form coordinates.

3. A Pendulum with an elastic string with a length of one meter, tunes $\nu_x = 0.17$, $\nu_y = 0.91$, and emittances of 3000πmm mrad. The motion of this system is completely stable for small enough energies, since the energy is a Lyapunov function.
4. As an example for a storage ring, we used the ring at IUCF at Indiana University. The device is usually used for emittances of 0.3π mm mrad, which are made so small by electron cooling. Since we want to analyze operation without cooling, we assumed $\epsilon_x = 3.7\pi$mm mrad and $\epsilon_y = 2.2\pi$mm mrad. The linear tunes are chosen to be $\nu_x = 0.7727$ and $\nu_y = 0.6650$.
5. A second example storage ring is the PSR II, which was designed as a possible upgrade of PSR at LAMPF in Los Alamos. It was analyzed for emittances of 40πmm mrad and linear tunes $\nu_x = 0.2313$ and $\nu_y = 0.2705$.
6. A custom made ring for demonstration purposes called the DEMO ring. This is a simple example ring for medium energy nuclear physics. It was analyzed for emittances of $\epsilon_x = 5\pi$ mm mrad $\epsilon_y = 7\pi$ mm mrad The linear tunes are $\nu_x = 0.37$ and $\nu_y = 0.67$.

5 PARAMETERIZING REGIONS AND CHOOSING THE PSEUDO INVARIANT

Describing the initial $\mathcal{O}$ region and the allowed region $\mathcal{A}$ is essential to finding $\mathcal{S}_i$ and $\mathcal{S}_f$ and therefore to finding a function that changes substantially between those two regions. Accelerators usually have mid–plane symmetry, which implies that the linear map does not couple the x–p_x and y–p_y component of motion. The projection

of the linear motion of beam particles in the x–p_x subspace lies on invariant ellipses. The area of these ellipses are called the x and y emittances of the beam. Since the product of two ellipses is topologically a torus, the linear motion is said to lie on an invariant torus. The allowed region for a beam in a storage ring is typically given by the acceptance in the x–p_x and the y–p_y phase space.

The rotations in nonlinear normal form theory correspond to rotations on the invariant ellipses. It is therefore natural that in a nonlinear theory the allowed region or nonlinear acceptance $\mathcal{A}$ should be given by a nonlinear invariant of the map, which can be computed by normal form theory. Normal form theory gives one invariant circle for each of the d degrees of freedom.

The pictures (a) and (b) in Fig. 3 describe the nonlinear invariants which specify the boundary of the allowed region. Since the linear contribution in the map dominates, they are close to invariant ellipses of linear motion.

There is a multitude of invariant surfaces which can be constructed from the d nonlinear invariants I_i. Two obvious choices are

$$\mathcal{A}_\circ = \{\vec{z} | \sum_{i=1}^{d} \frac{I_i(\vec{z})}{\epsilon_i} \leq 1\} , \tag{6}$$

$$\mathcal{A}_\square = \{\vec{z} | \max\{\frac{I_i(\vec{z})}{\epsilon_i}, i \in \{1, \ldots, d\}\} \leq 1\} . \tag{7}$$

The corresponding beam shape is displayed in Fig. 3(c) by drawing the largest allowed x and y coordinates. Elliptic beam shapes correspond to $\mathcal{A}_\circ$, and rectangular beam shapes correspond to $\mathcal{A}_\square$. To keep the notation simple, we describe the initial region $\mathcal{O}$ in a similar way with nonlinear emittances $\alpha\epsilon_i\pi$, where $\alpha < 1$. The boundaries are most easily described when a norm is introduced which measures the distance from the closed orbit according to the invariant torus on which the particle moves in n^{th} order approximation. If we want to represent the beam by a round shape, we choose $||\vec{z}||_\circ$, while if we want to describe it by a rectangle, we choose $||\vec{z}||_\square$, where

$$||\vec{z}||_\circ = \sum_{i=1}^{d} \frac{I_i(\vec{z})}{\epsilon_i} , \quad ||\vec{z}||_\square = \max\{\frac{I_i(\vec{z})}{\epsilon_i}, i \in \{1, \ldots, d\}\} . \tag{8}$$

A point in normal form space is characterized by the radii I_i and phases ϕ_i. The surface in normal form space, on which all points have the radii I_i, is a pseudo invariant torus. Nonlinear normal form theory leads to the transformation $\vec{B}$ from phase space to normal form space. The inverse transformation can be computed up to order n and is called the order n inverse $\vec{B}^{-1,n}$. The relevant phase space regions $\mathcal{O}$ and $\mathcal{A}$ can be constructed from tori in normal form space. The order n inverse transforms these tori in normal form space to areas in phase space.

$$\mathcal{T}(\vec{\epsilon}) = \{\vec{B}^{-1,n}(\vec{z}) | \begin{pmatrix} z_{2i-1} \\ z_{2i} \end{pmatrix} = \sqrt{\epsilon_i} \begin{pmatrix} \cos(\phi_i) \\ \sin(\phi_i) \end{pmatrix}, \phi_i \in [0, 2\pi], \forall i \in \{1, \ldots, d\}\} . \tag{9}$$

With this notation we can introduce regions in phase space which can describe the initial region $\mathcal{O}$ and the allowed region $\mathcal{A}$. Let

$$\mathcal{F}_\circ(\xi,\zeta) = \{\vec{z}|\vec{z}\in\mathcal{T}(\vec{\eta}),\xi\le\sum_{i=1}^{d}\frac{\eta_i}{\epsilon_i}\le\zeta\}\ , \tag{10}$$

$$\mathcal{F}_\square(\xi,\zeta) = \{\vec{z}|\vec{z}\in\mathcal{T}(\vec{\eta}),\xi\le\frac{\eta_i}{\epsilon_i}\le\zeta,\forall i\in\{1,\ldots,d\}\}\ , \tag{11}$$

then the regions of interest are given by

$$\mathcal{O}_s=\mathcal{F}_s(0,\alpha)\ ,\quad \mathcal{A}_s=\mathcal{F}_s(0,1)\ ,\quad s\in\{\circ,\square\}\ . \tag{12}$$

If $\vec{B}^{-1,n}$ were an exact inverse of $\vec{B}$, then $\mathcal{F}_s(0,1)$ would be exactly equal to the regions of equation (6) and (7), which can be described by $||\vec{z}||_s\le 1$. Since $\vec{B}^{-1,n}$ is an order n inverse of $\vec{B}$, $\mathcal{F}_s(0,\zeta)$ is approximately the same as $||\vec{z}||_s\le\zeta$. Therefore, the pseudo invariant $||\vec{z}||_s$ fluctuates very little on the surfaces of $\mathcal{O}_s$ and $\mathcal{A}_s$ as specified in equation (12). Phase space points in the regions of interest are easily parameterized by ϕ_i and η_i.

It is worthwhile to note that the first order inverse $\vec{B}^{-1,1}$ is the exact inverse of the first order of $\vec{B}$, and thus $\vec{B}^{-1,1}$ transforms circles into invariant ellipses of linear motion. Therefore, when $n=1$ is chosen in equation (9), the conventional linear definition of the acceptance is obtained. Since the polynomial map $\vec{B}^{-1,n}$ is continuous, it maps closed regions of normal form space into closed regions of phase space. Therefore, this definition of the acceptance is intuitive; particles can never leave the region of $\mathcal{F}_s(0,\zeta)$ without crossing the surface $\mathcal{F}_s(\zeta,\zeta)$.

To make the desired estimate as large as possible, we should find a function f which tends to increase when $||\vec{z}||_s$ increases and should at the same time be close to an invariant to make δ in equation (3) as small as possible. The appropriate choice is $f_\circ(\vec{z})=||\vec{z}||_\circ$ and $f_\square(\vec{z})=||\vec{z}||_\square$.

There are three reasons which suggest the use of $f_\circ$. First, for d degrees of freedom, evaluating $f_\square$ takes d times longer than evaluating $f_\circ$, since d pseudo invariants have to be evaluated, whereas for $f_\circ$, the polynomials I_i/ϵ_i given by normal form theory can be summed before evaluation. Second, since the beamline is generally circular, it seems more appropriate to choose $f_\circ$, which leads to elliptic rather than rectangular beam shapes. In the following the quantities with the circular subscript will be used and the subscript will be dropped.

6 ANALYSIS OF PSEUDO INVARIANTS

The PIE method relies on the choice of the function f, which should change little under application of the map $\vec{M}$. In order to show how little the order $n+1$ pseudo invariants of the normal form transformation change under application of $\vec{M}$, the six systems described in section 4 were analyzed. In Fig. 4 the deviation function $d_f=f(\vec{M})-f$ of the pseudo invariant f is plotted. The coordinate axes in the

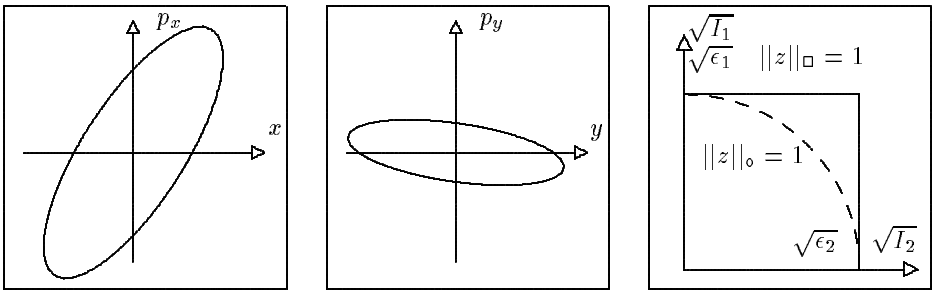

FIGURE 3: The motion on nonlinear invariants in the phase space section x–p_x is depicted in the left figure (a) and y–p_y in the middle figure (b). The allowed and the forbidden region and the definition of $||\vec{z}||$ is depicted in the right figure (c).

upper left picture are polar coordinates $(\sqrt{\epsilon}, \phi)$ for the Henon map. The other three examples are systems for four dimensional phase space. Therefore, the invariant defect is depicted on a torus $\mathcal{T}(\vec{\epsilon})$. The coordinates in the figures are the angles ϕ_1 and ϕ_2 which parameterize this surface. When comparing the accuracy of the coupled pendulum to the other systems, it should be noted that the emittance of the pendulum is about 1000 times larger. The accuracy of the pendulums pseudo invariant is only possible because the physical pendulum has an exact invariant.

Up to tenth order, the resonance denominators $D_l(\vec{k})$ for the two systems with one degree of freedom are bounded below in magnitude by 0.1. For two degrees of freedom the resonance denominators up to order ten have absolute values which exceed 0.001 and are sufficiently large to avoid divisions by dangerously small numbers. However, the normal form transformation requires successive divisions by these denominators, and after multiple divisions, very big and inaccurate coefficients can occur in the normal form transformation. Any computational errors therefore may have a negative influence on the quality of the pseudo invariant, but they have no influence on the rigor of the long term estimate; the estimate only becomes more pessimistic.

7 INFLUENCE OF RESONANCES

In general a normal form transformation is only possible if no resonance condition up to order n is satisfied. We therefore have to face the fact that resonances up to evaluation order have to be avoided in order to perform the normal form transformations needed for the PIE method.

If the tunes are close to a resonance condition, small denominators $D_l(\vec{k})$ occur in the normal form calculation, the transformation becomes inaccurate and the quality of the pseudo invariant decreases. This decrease is not only a computational problem but it has physical reasons, since at resonances good pseudo invariants do not exist.

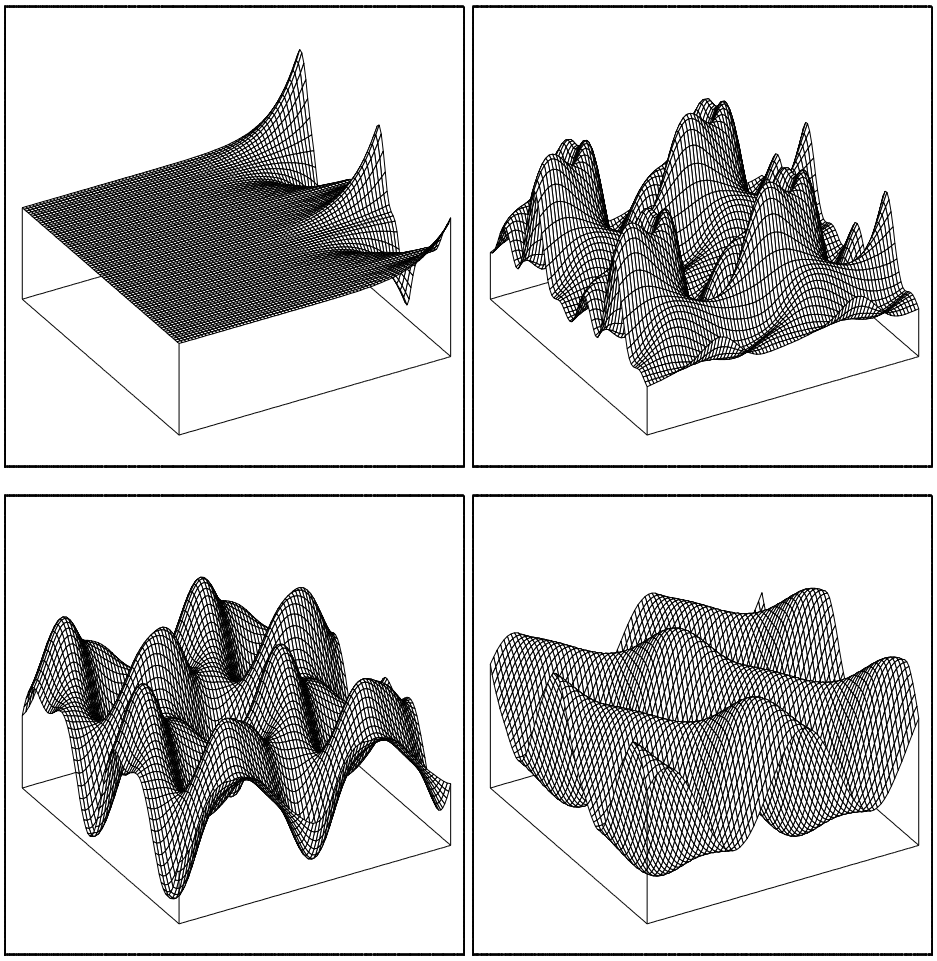

FIGURE 4: From left to right and top to bottom the invariant defect d_f is shown for: Henon map, Coupled pendulum, IUCF ring, and PSR II ring. The range of the depicted functions is $[-2.55 \cdot 10^{-13}, 7.36 \cdot 10^{-13}]$, $[-6.84 \cdot 10^{-9}, 6.00 \cdot 10^{-9}]$, $[-1.76 \cdot 10^{-9}, 1.65 \cdot 10^{-9}]$, and $[-7.2210^{-9}, 6.95 \cdot 10^{-9}]$.

To analyze this fact, we computed the effect of the tune on the pseudo invariants and thus on the long term estimates of the PIE method. For the Pendulum and the Henon map, we scanned the tune in 200 steps from 0 to 1. The variation of the deviation function is recorded in Fig. 5(a), where a logarithmic scale was used. The rapidly increased deviation from invariance and thus the rapidly decreased survival times close to tune resonances can be clearly seen for every single resonance up to order eight, the evaluation order of the normal form transformation. This figure suggests the well known fact that it is advisable to keep the tune of storage rings away from resonances.

For the pendulum, normal form theory can be used to approximate the exact invariant given by the Hamiltonian. This works even when the resonance denominators vanish[20].

Fig. 6 shows a corresponding picture for the deviation function of the PSR II ring and the DEMO ring. Calculations were performed to order 8. The tunes ν_x and ν_y were scanned from 0 to 1 in 100×100 steps. In order to obtain comparable systems the maps were computed and then composed with a linear map to obtain a symplectic map with the desired tunes. Again the figure is shown with a logarithmic scale. The boundary of the tune space has zero tune and is therefore excluded.

Susceptibility to resonances up to order five can be observed in the case of the DEMO ring; however, it is also apparent that not all resonances are observed, which is a consequence of the specific design features of the ring. The figures suggest that such plots of survival time versus tune of this or a similar kind can be helpful for machine analysis and optimization in the future, and it appears that more experience with this technique may lead to rather detailed predictions.

8 SYMPLECTIC REPRESENTATIONS

The fact that the normal form method yields invariants hinges critically on the symplecticity of the map. This fact and also the observation that symplecticity guarantees area conservation in phase space naturally suggests to impose symplecticity on transfer maps describing accelerators. This can be done in a variety of ways, the simplest of which is probably an increase in the computation order to a level where the error in symplecticity is substantially reduced. Another way is based on computing an order n generating function for the transfer map[25,26,27].

While for purposes of tracking based on the repeated application of maps, symplectification usually improves the long-term qualitative accuracy, for the case of the PIE method which relies entirely on applying the map only once, any symplectification of the map does not appear advantageous ad hoc. To study this issue, both the method of attaining symplecticity by higher evaluation orders as well as that based on generating functions were studied for the six sample problems under consideration.

In all cases symplectification does not offer any advantages over the direct use of the transfer map, and in most cases, the invariant defect d_f of the pseudo invariants is actually larger after symplectification. Tab. 1 shows the invariance defect

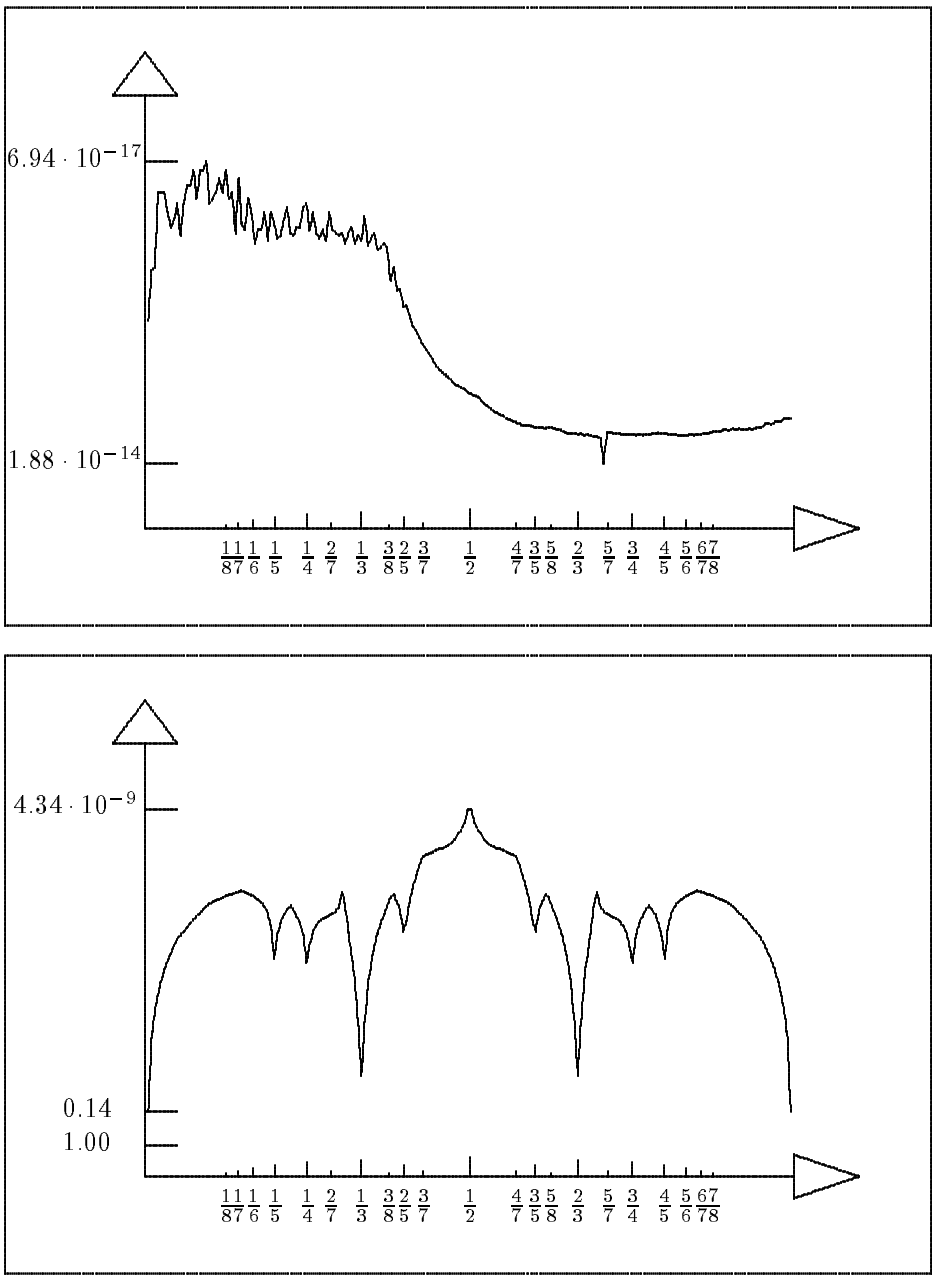

FIGURE 5: Variation of the maximum δ of the deviation function d_f with tune for a pendulum and the Henon map. The scale is logarithmic and inverted. Staying away from resonances yields long survival time predictions with PIE.

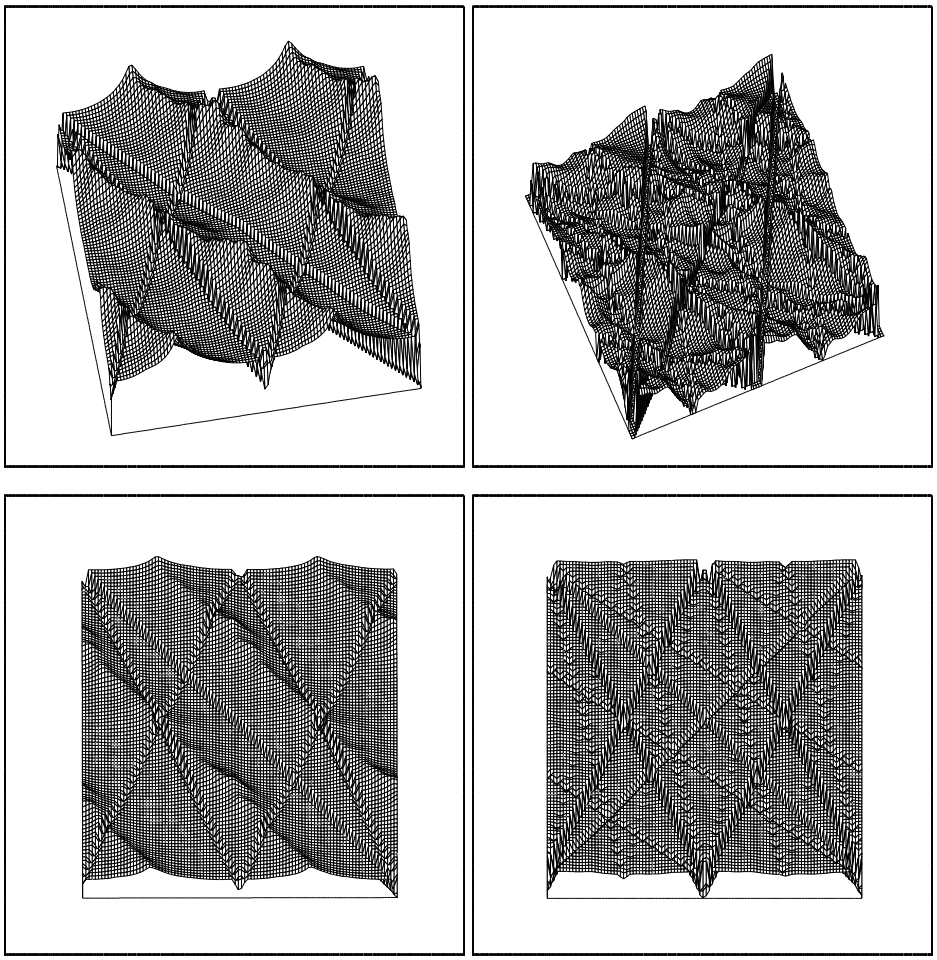

FIGURE 6: Variation of the maximum δ of the deviation function d_f with tune for the 8^{th} order map of the PSR II (two pictures left) and of the DEMO ring (two pictures right). The scale is logarithmic and inverted. The whole horizontal and vertical tune space is covered: $\nu_x \times \nu_y \in [0,1] \times [0,1]$. The range of d_f is from $2.2 \cdot 10^{-10}$ to $1.9 \cdot 10^{-7}$ (left) and from $1.3 \cdot 10^{-9}$ to $1.9 \cdot 10^{-4}$ (right).

of the coupled pendulum for the 9^{th} order polynomial f for symplectification by evaluating the map to various orders. The quality of the invariants does not change substantially since the first 9 orders cancel with and without this kind of symplectification.

TABLE 1: Maximum of the deviation function after symplectifying the map by adding higher orders.

Order	Coup. Pend. (10^{-13})	IUCF (10^{-9})	PSR II (10^{-9})	Demo (10^{-9})
8	5.858924	5.746786	1.597229	8.808577
9	9.721390	5.717355	1.599737	9.759362
10	9.677259	5.721978	1.599741	9.735593
11	9.744150	5.722880	1.599745	9.137200
12	9.745815	5.722909	1.599745	9.867690

It may be expected that symplectification may have an advantage once the invariant defect is studied for repeated application of the map. However, for turn numbers up to 100 studied here, such an effect is not observed, and again the non-symplectified transfer map yields a more favorable invariant defect as shown in Tab. 2.

TABLE 2: The maximum of the deviation function for different numbers of turns N when the map is represented by a generating function F_1 or by the Taylor map $\vec{M}$.

	C. Pen. (10^{-14})		IUCF (10^{-11})		PSR II (10^{-10})		Demo (10^{-13})	
N	F_1	$\vec{M}$	F_1	$\vec{M}$	F_1	$\vec{M}$	F_1	$\vec{M}$
10	293	276	881	823	126	115	122581	129261
20	534	508	969	988	232	223	97341	87990
30	723	705	1191	1496	321	310	77279	67182
40	866	840	1091	1396	379	373	21238	36807
50	1002	949	1497	1219	462	449	43855	61792
60	1232	1214	1178	1334	571	561	128	125
70	1476	1444	1427	1028	674	666	162	153
80	1656	1637	1187	934	761	754	172	177
90	1803	1778	859	1134	820	814	194	186
100	1941	1890	1007	721	856	853	209	210

9 SIMPLIFICATIONS

In section 4 four problems were mentioned. The first problem, finding a suitable pseudo invariant f, has been discussed. The remaining three problems are connected to finding the minimum of f on $\mathcal{S}_f$, the maximum of f on $\mathcal{S}_i$, and the maximum of d_f on $\mathcal{A}\backslash\mathcal{O}$. The regions $\mathcal{S}_i = \vec{M}(\mathcal{O})\backslash\mathcal{O}$ and $\mathcal{S}_f = \vec{M}(\mathcal{A})\backslash\mathcal{A}$ cannot be represented as clearly as the regions $\mathcal{O}$ and $\mathcal{A}$. This does not lead to a problem when phase space regions are used which contain $\mathcal{S}_i$ and $\mathcal{S}_f$. When the maximum $\delta_\mathcal{O}$ of the deviation function on $\mathcal{O}$ and the maximum δ on $\mathcal{A}\backslash\mathcal{O}$ is known, it is sufficient to choose

$$\mathcal{S}_i = \mathcal{F}(\alpha, \alpha + \delta_\mathcal{O}) \ , \quad \mathcal{S}_f = \mathcal{F}(1, 1 + \delta) \tag{13}$$

with the phase space domain $\mathcal{F}(\xi, \zeta)$ defined in equation (10).

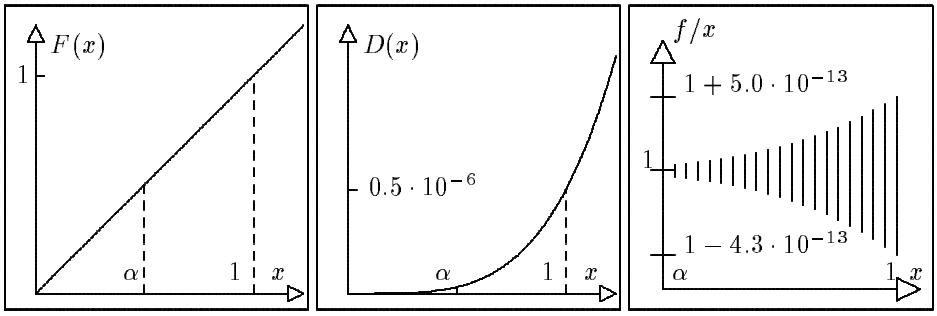

FIGURE 7: The left figure (a) depicts $F(x)$ and the middle figure (b) shows $D(x)$ in the allowed region. The variation of the pseudo invariant f on the phase space region $\mathcal{F}(x, x)$ is shown in the right figure (c).

The functions f and d_f have some properties which allow sensible simplifications. Those properties will be demonstrated for the proposed PSR II. Here the evaluation order is 6 and the acceptances are $\epsilon_i = 100$mm mrad. As shown in Fig. 7(a), the function $F(x) = \max\{f(\vec{z})|\mathcal{F}(x, x)\}$ is typically growing monotonously with x so that the maximum of $f(\vec{z})$ on $\mathcal{S}_i$ occurs on the surface $\mathcal{F}(\alpha + \delta_\mathcal{O}, \alpha + \delta_\mathcal{O})$, which is approximately described by $||\vec{z}|| = \alpha + \delta_\mathcal{O}$; and the minimum of $f(\vec{z})$ on $\mathcal{S}_f$ occurs on the surface $\mathcal{F}(1, 1)$ of $\mathcal{A}$, where $||\vec{z}||$ is approximately 1. The function $D(x) = \max\{d_f(\vec{z})|\mathcal{F}(x, x)\}$ is also typically growing monotonously as shown in Fig. 7(b). Therefore, the maximum δ typically occurs close to the border of the allowed region, where $||\vec{z}||$ is approximately 1. Furthermore, Fig. 7(c) shows that the variation of $f(\vec{z})$ on $\mathcal{S}_i$ and $\mathcal{S}_f$ is much smaller than $\Delta f = f_f - f_i$ which therefore is close to $1 - \alpha$. We obtain the estimate

$$N = \frac{1 - \alpha}{\max\{d_f(\vec{z})|\mathcal{F}(1, 1)\}} \ , \tag{14}$$

which involves finding only one maximum on a subspace with nearly constant $||\vec{z}||$. The Fig. 4 in section (6) shows the range of the functions d_f on the border of the allowed region $\mathcal{A}$ for all the example systems. The functions d_f do not have sharp maxima so that sampling with 20 steps in each direction gives a good approximation of the maximum value. Tab. 3 displays N for different systems and for different evaluation orders for $\alpha = 1/2$. Due to energy conservation, the pendulum and the coupled pendulums are stable for all times. The quality of our estimate is shown by the large numbers N which we obtain for those cases, in spite of the fact that the emittances are large and nonlinearities are quite important.

TABLE 3: Minimum number of turns required to move from the initial region to the forbidden region. The initial emittance was chosen to be half the acceptance. The maps were evaluated in order eight, whereas the pseudo invariants were computed to the indicated order. Scanning was performed with 20^k points for $k \in \{2, 4\}$ relevant dimensions.

Order	**Pendulum**	**Henon Map**	**Coupled Pendulums**
2	434	6	43
3	434	41	915
4	1,039,578	1,109	85,907
5	1,039,578	7,149	2,577,221
6	455,537,706	27,556	61,418,923
7	455,537,706	176,827	1,535,527,685
8	92,114,163,553	1,474,124	29,750,319,370
9	92,114,163,553	9,133,037	357,584,630,384
Order	**IUCF**	**PSR II**	**Demo**
2	9	806	6
3	321	831	129
4	1,288	252,893	1,220
5	19,995	235,650	25,657
6	370,294	6,977,545	84,087
7	3,265,268	8,255,710	1,320,751
8	11,277,884	65,472,668	4,554,994
9	65,734,218	76,092,850	55,548,695

10 REFINEMENTS AND EXAMPLES

Two methods will be introduced that increase the quality of the bounds on long term stability. One is connected to separating phase space in appropriate regions, the other involves multi–turn maps. Furthermore, unknown parameters of the system will be included in the estimates. The results for the six example maps are

accumulated in Tab. 5. In this table the guaranteed number of turns is given for the assumed acceptance $\epsilon\pi$, which is specified in section (4) for each system, and an initial beam with emittance $\epsilon\pi/2$. For the coupled pendulum and for the IUCF ring, the emittance for which a beam can be guaranteed to survive 10^8 turns is also shown.

10.1 Dividing Phase Space

Because δ usually increases rapidly with increasing $||\vec{z}||$, it is appropriate to separate the regions between $||\vec{z}|| = \alpha$ and $||\vec{z}|| = 1$ by surfaces $\mathcal{F}(\alpha_i, \alpha_i)$, $i \in \{0, \ldots, k\}$, where $\alpha_0 = \alpha$ and $\alpha_k = 1$. With $u_i = \max\{f(\vec{z})|\vec{z} \in \mathcal{F}(\alpha_i, \alpha_i)\}$ and $l_i = \min\{f(\vec{z})|\vec{z} \in \mathcal{F}(\alpha_i, \alpha_i)\}$ a lower bound on the number of turns can then be obtained from

$$N = \sum_{i=1}^{k} \frac{l_i - u_{i-1}}{\delta_i} \text{ with } \delta_i = \max\{d_f(\vec{z})|\mathcal{F}(\alpha_i, \alpha_i)\} \ . \tag{15}$$

The turn numbers obtained from this technique and the transportable emittances are given in Tab. 5 in the third line. In our experience this separation of phase space can improve the estimate by up to an order of magnitude.

The potential of this approach can be seen when using

$$D(x) = \max\{d_f(\vec{z})|f(\vec{z}) = x\} \ . \tag{16}$$

We estimate the change that occurs in x by k map applications as $x(n+k) - x(n) = D(x(n+k)) \cdot k$ and approximate for big turn numbers N as

$$N(x) = \int_{\alpha}^{x} \frac{d\tilde{x}}{D(\tilde{x})} \ . \tag{17}$$

In Fig. 8 $N(x)$ corresponds to the area under the curve. The PIE method without dividing phase space, however, only gives the area in the rectangle as guaranteed survival time.

10.2 Educated Lumping

The largest change that can be generated by N applications of the map is usually much smaller than N times the largest growth that can happen during a single turn. Therefore, it is advantageous to consider the maximum growth that can occur when the map is applied several times. One can furthermore carefully choose the proper number of turns such that the estimates become most favorable.

In order to find the optimum number of map applications the maximum and minimum of $d_f(\vec{z})$ over the allowed region $\mathcal{A}$ was plotted for many turns. The Figs. (9a–f) display the variation of $d_f(\vec{z})$ for our examples. For the improvements illustrated in Tab. 5, the number of map applications used are displayed in Tab. 4.

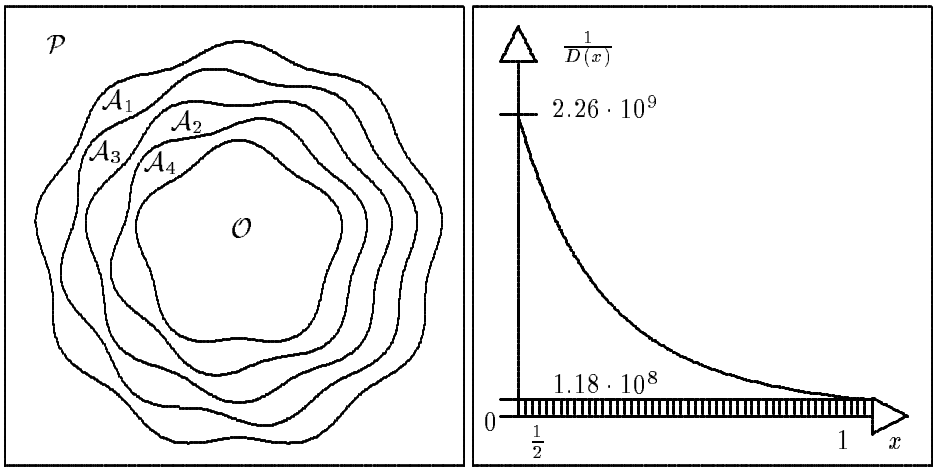

FIGURE 8: Dividing phase space (left) approximates the area under the displayed curve (right) by several rectangles to obtain the bound on the survival time. Without this improvement the PIE method would only give the area of the dashed rectangle.

TABLE 4: Number of map applications used for improving the estimation.

Pend.	**Henon**	**Coup. Pend.**	**IUCF**	**PSR II**	**DEMO**
14	37	6	89	247	100

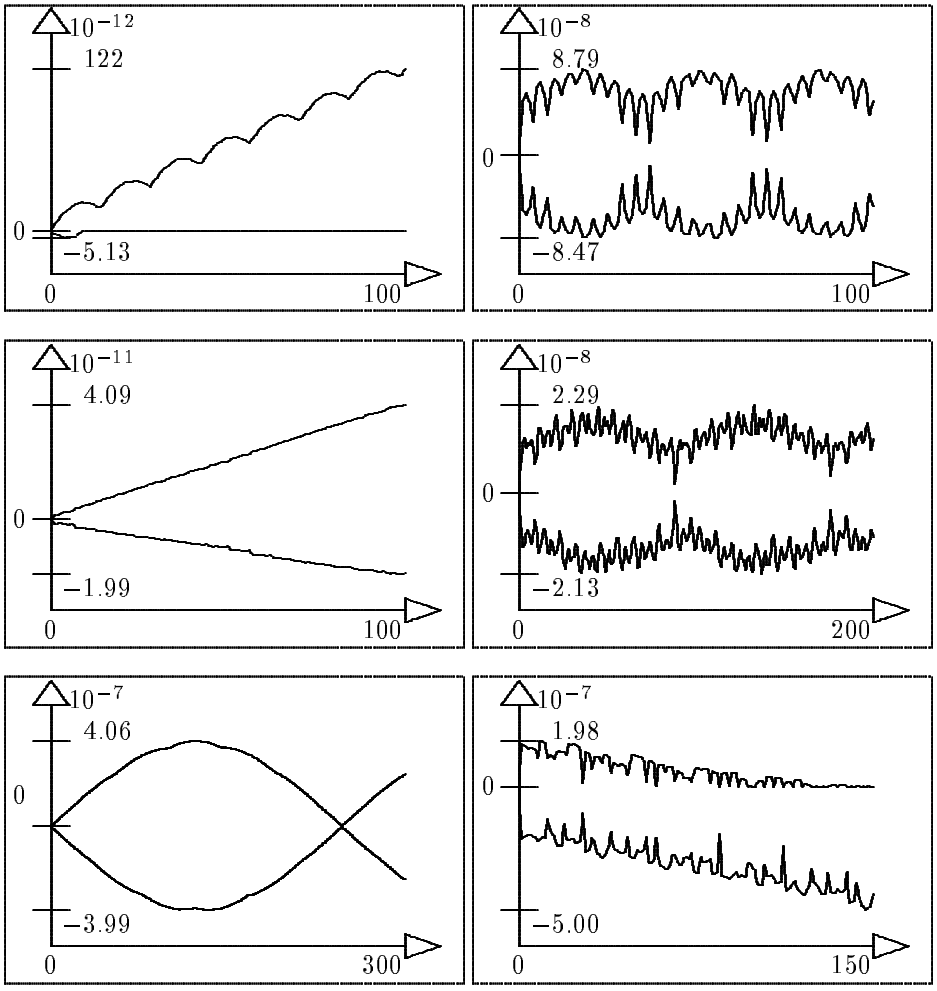

FIGURE 9: The figures display the variation of the deviation function d_f in the allowed region for the six examples. From left to right and top to bottom these are (a) Pendulum, (b) Henon map, (c) Coupled pendulum, (d) IUCF, (e) PSR II, (f) Demo.

10.3 Parameter Dependences

So far, the normal form method assumes that the one–turn map of the storage ring in question is well known. Since this is rarely the case, the theory has been extended to maps which depend on an unknown parameter, which could be the particle's energy or some magnet parameters. We computed the map as a function of a parameter of interest and then scanned not only through the relevant region of phase space, but also through the range for the parameter.

If the map $\vec{M}$ is a function of a parameter, then the nonlinear normal form transformation $\vec{B}$ also depends on a parameter. Using DA programs allows to compute the Taylor expansion of this parameter dependent map $\vec{B}$. The pseudo invariant f then also depends on the parameter. Changing the parameter changes the transfer map and the pseudo invariant simultaneously, such that f stays a good pseudo invariant for a wide range of the parameter. This is apparent when one considers that to order $n+1$,

$$f \circ \vec{M} - f =_{n+1} 0 \tag{18}$$

also holds to for parameter dependent normal form transformations.

11 OUTLOOK: RIGOROUS PIE WITH INTERVAL ARITHMETIC

Experience shows that the described method usually gives a very reliable lower bound on the number of stable turns. However, the method can even be extended to make completely certain statements about bounds in a mathematically rigorous sense. This requires a rigorous execution of several individual steps; in particular, it is not sufficient to approximate the maximum of δ by scanning.

In practice it turns out that standard methods of interval arithmetic commonly used for verified global optimization [28] are not suitable for the complicated functions d_f at hand because of the tremendous blow-up caused by the complexity of the underlying algorithm. A novel combination of DA methods with interval methods called Remainder Differential Algebra (RDA) allows not only the computation of Taylor expansions of arbitrary functions, but also a rigorous error bound of the expansion under consideration[23]. A predecessor of the method that can already successfully solve part of the questions at hand is the so-called Interval Chain approach[20,21]. The RDA method for the first time allows to make fully rigorous statements on the survival times of particles in circular accelerators and other weakly nonlinear dynamical systems.

TABLE 5: Lower bounds on the number of turns which particles survive for an initial emittance of one half the acceptance and lower bounds on the stable emittances for 10^8 turns obtained by various variations of the PIE method.

Lower bound for	**Pendulum**	**Henon map**
Simplest application	92,114,163,553	9,133,037
Length and Strength vary by 1%	23,556,300,993	8,167,533
Divided phase space	452,868,876,965	44,999,781
Multi–turn maps	388,804,862,856	1,456,171,297
Both	1,895,348,117,634	4,779,711,057
Lower bound for	**PSR II**	**Demo**
Simplest application	76,092,850	55,548,695
Quad field varies by 0.01%	47,166,060	51,963,620
Divided phase space	373,642,327	284,008,517
Multi–turn maps	21,172,838,624	1,042,575,616
Both	18,731,455,785	5,121,716,506
Coup. Pendulum	predicted turns	stable emittance
Simplest application	357,584,630,384	$5 \times 5\pi$m mrad
Length varies by 1%	144,173,434,143	$3.4 \times 3.4\pi$m mrad
Divided phase space	1,765,031,547,898	$11.3 \times 11.3\pi$m mrad
Multi–turn maps	1,029,815,934,687	$6 \times 6\pi$m mrad
Both	5,087,629,041,331	$14.5 \times 14.5\pi$m mrad
IUCF ring	predicted turns	stable emittance
Simplest application	65,734,218	$3.3 \times 2.0\pi$mm mrad
Quad field varies by 0.01%	18,535,102	$2.9 \times 1.7\pi$mm mrad
Divided phase space	335,420,083	$4.8 \times 2.9\pi$mm mrad
Multi–turn maps	5,804,832,818	$8.1 \times 4.8\pi$mm mrad
Both	27,745,480,680	$13 \times 7.7\pi$mm mrad

REFERENCES

1. N. N. Nekhoroshev. An exponential estimate of the time of stability of nearly–integrable Hamiltonian systems. *Uspekhi Mat. Nauk*, 32:6:5–66, 1977. and translation in Russian Mathematical Surveys 32:6, 1–65 (1977).
2. R. L. Warnock and R. D. Ruth. Long–term bounds on nonlinear Hamiltonian motion. *Physica D*, 56(14):188–215, 1992. also SLAC–PUB–5267.
3. J. S. Berg, R. L. Warnock, R. D. Ruth, and E. Forest. Construction of symplectic maps for nonlinear motion of particles in accelerators. Technical Report SLAC–PUB–6037, Stanford Linear Accelerator Center, 1993.
4. M. Berz. Differential Algebraic description of beam dynamics to very high orders. *Particle Accelerators*, 24:109–124, 1989.
5. Y. Yan. Success in one–turn maps for dynamic apperture studies – a brief review. In *Stability of Particle Motion in Storage Rings*, volume 292 of *AIP Conference Proceedings*, pages 177–181. AIP Press, 1994.
6. M. Berz. COSY INFINITY version 6 reference manual. Technical Report MSUCL-869, National Superconducting Cyclotron Laboratory, MSU, East Lansing, MI, 1992.
7. M. Berz. Automatic differentiation as nonarchimedean analysis. In *Computer Arithmetic and Enclosure Methods*, pages 439–450. Elsevier Science Publishers B.V., 1992.
8. H. Poincaré. *Les méthodes nouvelles de la méchanique céleste*. Gauthier–Villars, Paris, 1892, 1893, 1899. three volumes.
9. G. D. Birkhoff. Dynamical systems. *American Mathematical Society Publications*, 9, 1927.
10. C. L. Siegel. Über die Existenz einer Normalform analytischer Hamiltonscher Differentialgleichungen in der Nähe einer Gleichgewichtslösung. *Math. Ann.*, 128:144–170, 1952.
11. C. L. Siegel. *Vorlesungen über Himmelsmechanik*. Springer–Verlag, Berlin–Göttingen–Heidelberg, 1956.
12. A. N. Kolmogorov. On the conservation of conditionally periodic motions for a small change in the Hamiltonian. *Dokl. Akad. Nauk SSST*, 98:527–530, 1954.
13. V. I. Arnol'd. Proof of a theorem of A. N. Kolmogorov on the invariance of conditionally periodic motions under small perturbations of the Hamiltonian. *Uspekhi Mat. Nauk*, 18:5:91–192, 1963. and translation in Russian Mathematical Surveys 18:6, 85–191 (1963).
14. J. K. Moser. On invariant curves of area–preserving mappings of an annulus. *Nachr. Akad. Wiss. Göttingen, Math.–Phys. Kl. II*, pages 1–20, 1962.
15. G. Turchetti. Nekhoroshev stability estimates for symplectic maps and physical applications. In *Number Theory and Physics, Springer Proceedings in Physics 47*, Berlin, Heidelberg, 1990. Springer–Verlag.
16. R. L. Warnock, R. D. Ruth, W. Gabella, and K. Ecklund. Methods of stability analysis in nonlinear mechanics. Technical Report SLAC–PUB–4846, Stanford Linear Accelerator Center, 1989.
17. R. L. Warnock and R. D. Ruth. Bounds on nonlinear motion for a finite time. Technical Report SLAC–PUB–5020, Stanford Linear Accelerator Center, 1989.
18. R. L. Warnock and R. D. Ruth. Stability of orbits in nonlinear mechanics for finite but very long times. In *Nonlinear Problems in Future Accelerators*, pages 67–76, New York, 1991. World Scientific. also SLAC–PUB–5304.
19. R. L. Warnock. Close approximation to invariant tori in nonlinear mechanics. *Physical Review Letters*, 66(14):1803–1806, 1991.
20. G. H. Hoffstätter. *Rigorous bounds on survival times in circular accelerators and efficient computation of fringe–field transfer maps*. PhD thesis, Michigan State University, East Lansing, MI 48824, USA, 1994.
21. M. Berz and G. Heinz Hoffstätter. Exact bounds on the long term stability of weakly nonlinear systems applied to the design of large storage rings. *Interval Computations*, 2:68–89, 1994.
22. M. Berz and G. H. Hoffstätter. Rigorous lower bounds on the survival time in particle accelerators. *Particle Accelerators*, 54:193–202, 1996.

23. M. Berz and G. H. Hoffstätter. Computation and application of Taylor polynomials with interval remainder bounds. *Submitted to Interval Computations*, 1995.
24. M. Berz. Differential algebraic formulation of normal form theory. In *Proceedings of the 1992 Workshop on Nonlinear Effects in Accelerator Physics*, Berlin, 1992.
25. M. Berz. Differential Algebraic treatment of beam dynamics to very high orders including applications to spacecharge. *AIP Conference Proceedings*, 177:275, 1988.
26. M. Berz. Symplectic tracking through circular accelerators with high order maps. In *Nonlinear Problems in Future Accelerators*, pages 288–296, New York, 1991. World Scientific.
27. M. Berz. Arbitrary order description of arbitrary particle optical systems. *Nuclear Instruments and Methods*, A298:426–440, 1990. also MSU–NSCL–1990/739.
28. E. Hansen. *An Overview of Global Optimization Using Interval Analysis*, pages 289–307. R. E. Moore, Academic Press, New York, 1988.